HHS Public Access

Author manuscript

Dev Biol. Author manuscript; available in PMC 2016 September 15.

Published in final edited form as:

Dev Biol. 2015 September 15; 405(2): 280–290. doi:10.1016/j.ydbio.2015.07.021.

Coordination between *Drosophila* Arc1 and a specific population of brain neurons regulates organismal fat☆

Jeremy Mosher[a], **Wei Zhang**[a], **Rachel Z. Blumhagen**[a], **Angelo D'Alessandro**[b], **Travis Nemkov**[b], **Kirk C. Hansen**[b], **Jay R. Hesselberth**[b], and **Tânia Reis**[a,*]

[a] Department of Medicine, Division of Endocrinology, Metabolism and Diabetes, University of Colorado Medical School, Aurora, CO 80045, United States

[b] Department of Biochemistry and Molecular Genetics, University of Colorado Medical School, Aurora, CO 80045, United States

Abstract

The brain plays a critical yet incompletely understood role in regulating organismal fat. We performed a neuronal silencing screen in *Drosophila* larvae to identify brain regions required to maintain proper levels of organismal fat. When used to modulate synaptic activity in specific brain regions, the enhancer-trap driver line E347 elevated fat upon neuronal silencing, and decreased fat upon neuronal activation. Unbiased sequencing revealed that *Arc1* mRNA levels increase upon E347 activation. We had previously identified *Arc1* mutations in a high-fat screen. Here we reveal metabolic changes in *Arc1* mutants consistent with a high-fat phenotype and an overall shift toward energy storage. We find that Arc1-expressing cells neighbor E347 neurons, and manipulating E347 synaptic activity alters Arc1 expression patterns. Elevating Arc1 expression in these cells decreased fat, a phenocopy of E347 activation. Finally, loss of Arc1 prevented the lean phenotype caused by E347 activation, suggesting that Arc1 activity is required for E347 control of body fat. Importantly, neither E347 nor Arc1 manipulation altered energy-related behaviors. Our results support a model wherein E347 neurons induce Arc1 in specific neighboring cells to prevent excess fat accumulation.

Keywords

Arc; Neuronal regulation of obesity; Genetics; Fat; Brain

1. Introduction

Organisms usually strive for energy equilibrium, with uptake balanced by expenditure and storage. Excess energy storage as triglycerides leads to human obesity, accompanied by increased susceptibilities to many diseases (Guh et al., 2009). In mammals, tissues responsible for the majority of fat storage (white adipose) are distinct from those where fats

☆GEO database access: ⟨http://www.ncbi.nlm.nih.gov/geo/query/acc.cgi?token=qzcnyucqzxerlgn&acc=GSE60822⟩.

*Correspondence to: 12801 E 17th Ave, MS 8106, Aurora, CO 80045, United States. tania.reis@ucdenver.edu (T. Reis)..

Appendix A. Supplementary material

Supplementary data associated with this article can be found in the online version at http://dx.doi.org/10.1016/j.ydbio.2015.07.021.

are synthesized *de novo* (liver) or incorporated from dietary sources (gut), requiring coordination via circulating signals. Additionally, centralized control of the behavioral components of energy homeostasis (food choice, feeding rates, locomotor activity), as well as direct regulation of metabolic processes (e.g., breakdown of storage molecules), occur in the brain (Morton et al., 2006).

In principle, energy imbalance caused by misregulation at any of these levels could predispose to obesity. Strikingly, a genome-wide association study identified 11 obesity-associated loci, many of which contain genes that are highly expressed in the brain (Thorleifsson et al., 2009). These data point to the brain as a key regulator of metabolic function, and highlight the need for improved understanding of the pathways by which the brain maintains energy homeostasis.

Invertebrates with simplified central nervous systems (CNSs) are attractive models for the study of roles for the brain in energy balance. *Drosophila melanogaster* has emerged as a powerful model for both metabolism (Baker and Thummel, 2007) and central regulation of behavior (Anholt and Mackay, 2012; Davis, 2011; Kaun et al., 2012; Scott, 2005; Yamamoto and Koganezawa, 2013). Unbiased genetic screens have identified brain-expressed *Drosophila* genes whose function prevents excess body fat (Pospisilik et al., 2010; Reis et al., 2010). Additionally, 350 lines driving heterologous gene expression in different subsets of neurons were screened for body fat levels following expression of a temperature-sensitive dynamin allele that blocks neurotransmitter uptake (Kitamoto, 2001), or a bacterial voltage-activated sodium channel (*NaChBac1*, or NB) that stimulates neuronal activity (Luan et al., 2006; Ren et al., 2001). This study identified two populations of adult brain neurons whose synaptic activity is required to prevent excess body fat accumulation, and sufficient to drive fat depletion (Al-Anzi et al., 2009). Numerous regions of the brain are represented in each of these populations, with very little overlap between the two (Al-Anzi et al., 2009). Accordingly, the specific neuronal groups and molecules responsible for these activities have yet to be determined.

We performed a similar screen focused on *Drosophila* larvae and here report results that differ from previous studies in several important ways. Larvae share major brain regions found in adults (Li et al., 2014) but exhibit a narrower range of behaviors focused on energy consumption, storage, and expenditure. We define a population of brain neurons that is necessary and sufficient for proper body fat storage, with no effect on food consumption or physical activity. We go on to identify the *Drosophila* homolog of Arc1 – an important synaptic effector protein (Bramham et al., 2010) – as a factor regulated by and required for these effects. Arc1 mutants display metabolic defects consistent with excess energy storage. These findings provide key insights into the functions of specific neurons in energy balance, and implicate Arc1 as an important factor in neuronal regulation of organismal metabolism.

2. Results

2.1. Regulation of Drosophila body fat by distinct groups of neurons in the larval brain

To identify brain regions required for energy balance in *Drosophila* larvae, we used a collection of 650 neuronal enhancer-trap GAL4 lines (generous gift of Ulrike Heberlein; see

(Gordon and Scott, 2009)) to overexpress a dominant-negative allele of *shibire* (*shi*^{DN}) (Moline et al., 1999), the *Drosophila* ortholog of dynamin, which prevents synaptic transmission. We screened these lines using a sensitive and robust density-based assay for larval body fat (Reis et al., 2010), and isolated 63 lines with a "floating" phenotype in combination with UAS-*shi*^{DN} (Table 1), suggestive of a requirement for those neurons in body fat regulation. In order to further characterize the brain regions necessary for body fat regulation, we crossed these driver lines with UAS-GFP and visualized the areas of the brain expressing GAL4 as reported by the GFP (Table 1 and Fig. S1). We noted enrichment for specific brain regions such as the pars intercerebralis (PI), mushroom body (MB), sub-esophageal ganglion (SOG) and ventral nerve cord (VNC). From these 63 lines we chose for further analysis 14 with representative and/or more restricted patterns of expression (Table 1). Since silencing of the neurons represented in these lines elevated body fat, we asked if increased neuronal activity of the same neuronal regions was sufficient to deplete body fat. To ask if neuronal activity is sufficient to deplete body fat, we used a UAS-linked transgene encoding the bacterial sodium channel NB to hyper-activate GAL4-expressing neurons (Luan et al., 2006; Ren et al., 2001). 7 of the 14 representative lines displayed a high-fat phenotype when the respective neuronal regions were silenced with *shi*^{DN} (Fig. 1A), and a lean phenotype when the same regions were stimulated with NB (Fig. 1A). These lines show expression in the MB, PI, SOG and VNC (Fig. S1, Fig. 3 and Table 1). Our results identify regions of the larval brain that are both necessary and sufficient for body fat regulation.

2.2. "E347" neurons are necessary and sufficient for fat regulation

Line E347 displayed a very strong "floating" phenotype upon functional silencing (Fig. 1A), and a "sinking" phenotype when stimulated (Fig. 1A). E693 caused even stronger phenotypes (Fig. 1A), but, unlike E347 (see below), E693 was also expressed in the main fat storage tissue, the fat body (FB) (data not shown). As we were most interested in neuronal functions in the brain, we focused on E347 for further study. Importantly, the E347 driver, *shi*^{DN}, or NB insertions alone caused no statistically significant difference in organismal fat as assayed by larval density (Fig. S2). We used the E347 driver as the genetic background control for the remainder of our experiments, and refer to the neurons that express GAL4 in this enhancer-trap line as E347 neurons.

We used gas chromatography/mass spectrometry (GC/MS) to confirm that neuronal silencing of E347 neurons elevated levels of all fatty acids in lipid extracts from whole larvae, increasing total neutral lipids (Fig. 1B). Body weight, which was used to normalize lipid content, was slightly but statistically significantly decreased (Fig. S3B). Thus, these animals have a higher proportion of fat despite a smaller overall mass. Notably, body size was not obviously different (Fig. S3D). We considered two possible explanations for the increased fat in the animals in which E347 neurons are silenced. First, extra fat might accumulate in all of the tissues where fat is normally stored. Second, extra fat could accumulate in tissues that do not normally accumulate stored fat. To visualize the tissue distribution of stored fat, we stained neutral lipids using Oil Red O, which provides a qualitative comparison of fat storage (Ramirez-Zacarias et al., 1992). The same tissues that accumulated neutral lipids in control animals expressing GFP from the E347 driver (FB, gut, imaginal tissues and epidermis to visualize the eonocytes) also contained neutral lipids in

animals expressing *shi*^{DN} from this driver (Fig. S3C). Thus, E347 silencing does not alter the distribution of fat storage. Interestingly, we did find that Oil Red O staining disappeared from a region of the gut in lean animals in which NB was expressed from the E347 driver (Fig. S3C). Decreases in fat stores upon E347 neuronal activation may thus result, at least in part, from changes in fat accumulation in specific tissues.

To address the cause of the elevated fat upon E347 silencing, we asked if there were defects in metabolic behaviors (feeding and physical activity). Excess stored energy could result from overeating. Indeed, other neuronal enhancer-trap lines identified in our high-fat screen exhibit overeating phenotypes upon neuronal silencing (T.R. unpublished data). However, levels of food consumption did not change when E347 neurons were less or more active, suggesting that caloric intake does not play a role in the associated fat phenotypes (Fig. S4A and B). Likewise, reduced physical activity could lead to excess fat storage. By placing larvae on an agar plate and analyzing videos of their subsequent activity during a defined period of time, we calculated larval velocities. Other neuronal enhancer-trap lines examined with this assay displayed significant alterations in physical activity (T.R. unpublished data). However, for E347 neurons this assay also showed no differences between average velocities in either condition (Fig. S4C and D).

While we set out to investigate roles for specific regions of the brain in body fat regulation, we considered the possibility that manipulation of neuronal activity in non-brain neurons via *shi*^{DN} or NB expression from the E347 driver could be responsible for the observed fat phenotypes. We therefore used the E347 driver to express a GFP reporter, and stained fixed tissues for Elav as a neuronal marker (Campos et al., 1987). In addition to strong signal in specific regions of the brain (see below for more detailed analysis), we detected GFP in a few cells in the gut and imaginal wing, halter and leg discs (Fig. S5). However, only in the brain was there significant overlap between GFP and Elav expression (Fig. S5). We therefore focused on the regulation of body fat by E347-expressing neurons in the brain.

2.3. Arc1 mRNA is upregulated in brains where E347 neurons are stimulated

In order to identify specific molecules involved in this metabolic regulation, we isolated mRNA from control brains or those in which E347 neuronal activity was silenced or activated, and measured RNA abundance by RNAseq. In this analysis, we identi-fied 46 genes that changed significantly comparing the silencing versus induction conditions. We found that Arc1 was the second-most elevated mRNA (2.7-fold). Arc1 is a conserved activity-regulated immediate early gene that we had previously isolated in an unbiased screen for fat mutant larvae (Reis et al., 2010). RNAi-mediated depletion of Arc1 was also independently found in a high-throughput fat screen in adult flies (Pospisilik et al., 2010). However, nothing else is known about how Arc1 might function in the neuronal regulation of organismal metabolism. Arc1 thus represented a compelling candidate for a mediator of the organismal effects of manipulation of E347 neuronal activity.

Considering that Arc1 expression is known to increase upon synaptic activity (Mattaliano et al., 2007), upregulation of Arc1 upon NB overexpression could simply reflect synaptic stimulation. If so, other immediate early genes should also be upregulated in this condition to a similar extent. However, when comparing transcript levels from the E347/+ control to

E347 > NB, quantitative PCR (Fig. 2) revealed a much stronger induction of *Arc1* (fold induction 4.09±1.14–2.64±0.56) compared to two other immediate early genes, *jra* (fold induction 1.39±0.37–1.42±0.11) and kay (fold induction 1.18±0.17–1.48±0.29), the fly orthologs of jun and c-fos, respectively (Goldstein et al., 2001; Hudson et al., 2007), suggesting that Arc1 may play more specific effector roles in response to E347 activity.

2.4. Arc1 cells neighbor E347 neurons and respond to E347 neuronal activity

Using GAL4-mediated expression of GFP, we determined that E347 neurons are located in the middle region of the lobes of the larval brain, overlapping with the MB, SOG, optic lobes, and VNC (Fig. 3A). Arc1 induction upon stimulation of E347 neurons could reflect upregulation of Arc1 in E347 neurons themselves, or induction in neighboring cells triggered by E347 activity. To distinguish between these possibilities, we crossed E347 > GAL4 to a UAS-GFP line, dissected brains from the progeny and detected GFP and Arc1 protein in fixed tissues using specific antibodies. Arc1-expressing cells did not overlap with E347 neurons, but the two cell types were in very close proximity (Fig. 3A). These findings supported a model in which Arc1 upregulation occurs in non-E347 neurons in a manner dependent upon the activity of E347 neurons. To further test this model, we crossed our E347 > GAL4 UAS-GFP lines with either a w^{1118} control, a UAS-Shi^{DN} to prevent synaptic transmission, or a UAS-NB line to stimulate synaptic transmission, and performed immunostaining for GFP and Arc1. As immunostaining is not a particularly sensitive method with which to measure protein content per cell – indeed, we saw no apparent difference in Arc1 levels under the different conditions (data not shown) – we looked for changes in Arc1 expression by counting the number of clearly Arc1-positive cells in the different regions of the brain under the different conditions. The number of Arc1-expressing cells in the cluster of neurons previously reported to express Arc1 (Mattaliano et al., 2007) did not change upon neuronal silencing or stimulation of E347 neurons. However, we observed distinct clusters of Arc1-positive cells in different areas of the brain that seemed to respond to E347 neuronal activity. In agreement with the RNAseq and RT-qPCR data, we observed significantly more Arc1 cells in the VNC when E347 neurons were stimulated, and significantly fewer Arc1-positive cells were observed in the VNC and in the SOG upon E347 silencing (Figs. 3B, C and S6). Interestingly, we found more Arc1-positive peripheral (Per) lobe cells upon E347 neuronal silencing (Figs. 3B, C and S6), which likely explains why we failed to detect a reduction in overall Arc1 levels by RNAseq and RT-qPCR in this condition. We conclude that E347 neuronal activity modulates Arc1 expression in specific, distinct regions of the larval brain.

2.5. Arc1 is necessary and sufficient for body fat regulation

Arc1 levels change in opposing ways in neuronal conditions that result in opposing fat phenotypes. Accordingly, we hypothesized that Arc1 itself plays a critical role in neuronal regulation of body fat. Indeed, density analysis of animals carrying Arc1 null alleles compared to genetic-background controls demonstrated that loss of Arc1 decreases density, consistent with an increase in body fat (Fig. 4A). Oil Red O staining of Arc1 nulls and appropriate controls showed no change in the pattern of accumulation of neutral lipids in FB, gut, imaginal tissues or eonocytes (data not shown). To test if Arc1 overexpression is sufficient to prevent fat accumulation, we overexpressed Arc1 in Arc1-expressing cells

using a previously characterized Arc1 > GAL4 driver (Mattaliano et al., 2007). Arc1 overexpression resulted in a sinking phenotype (Fig. 4B). As we had observed upon manipulation of E347 neuronal activity, Arc1 mutation or overexpression did not affect food consumption or physical activity (Fig. S7). These findings are consistent with a model in which excess Arc1 depletes fat stores and/or prevents fat accumulation. To determine if neuronal Arc1 expression generally reduces fat storage, or, alternatively, if Arc1 must be expressed in specific neurons in order to carry out its fat-depleting function, we overexpressed Arc1 or depleted it via RNAi in E347 neurons. Neither manipulation had any effect on larval density (Fig. S8). Thus, Arc1 control of body fat regulation occurs in specific neurons. Moreover, Arc1 does not appear to simply modify the synaptic activity of the neurons in which it is expressed, because expression of Shi^{DN} or NB using the Arc1 > GAL4 driver had no effect on larval density (data not shown). We conclude that Arc1 plays a specific role in the fat-regulatory function of certain neuronal circuits.

2.6. Abnormal metabolic profiles in Arc1 mutants

To better understand the metabolic defects in *Arc1* fat mutants, we performed Ultra-High Performance Liquid Chromatography (UPLC)–MS-based metabolomic analysis in $Arc1^{18}$ versus $Arc1^{115}$ larvae. A total of 212 metabolites were monitored, as detailed in Supplementary Table 1. Partial least squares Discriminant Analysis (PLS-DA) confirmed the hypothesis that metabolic phenotypes were significantly divergent in $Arc1^{115}$ versus $Arc1^{18}$ larvae (Fig. S9). Specifically, high content analysis (HCA) of metabolic pathways and energy-related metabolites highlighted energy- and lipid metabolism-related pathways as the major differences discriminating the two groups (Fig. S10).

In light of these results, we decided to focus our analysis on central carbon metabolic pathways, including glycolysis, Krebs cycle and fatty acid oxidation/lipid synthesis (Fig. 5A). The glycogen breakdown products maltotriose and trehalose, as well as glucose, increased significantly in $Arc1^{18}$ larvae in comparison to $Arc1^{115}$ wt controls. However, this did not result in higher steady-state levels of downstream glycolytic intermediates and byproducts, such as glyceraldehyde 3-phosphate and pyruvate. Increases in the levels of glycerol-3-phosphate, the carbon backbone for esterification of storage di- and tri-acyl lipids, were also observed in $Arc1^{18}$ larvae. Decreases in the levels of acetyl-coA and citrate in $Arc1^{18}$ suggest that deregulation in late glycolysis might not be due to upregulation of the Krebs cycle. Both these observations and the accumulation of triphosphate, a substrate for *de novo* ATP synthesis, are suggestive of impaired energetics in $Arc1^{18}$ larvae. Increased levels of free carnitine and decreased levels of acetyl-carnitine are further indicative of decreased fatty acid catabolism. Decreased levels of free fatty acids, both short chain (butanoate) and long chain fatty acids (palmitate) are consistent with the sequestration of free fatty acids in storage lipids, consistent with our density assay results (Fig. 4A). We observed a strong (~5-fold) accumulation of aspartate in $Arc1^{18}$ larvae compared to $Arc1^{115}$ controls ($P < 0.0001$). Significant increases in the levels of branched chain amino acids (BCAA), phenylalanine and tyrosine were also observed (Supplementary Table 1).

To further highlight the metabolic defects of $Arc1^{18}$ mutants we extracted RNA and performed RT-qPCR to measure transcript levels of an array of metabolic enzymes. This

same panel of transcripts was previously used to illustrate the metabolic defects of *Sir2* mutant larvae, which accumulate excess fat due to a metabolic switch to energy storage (Reis et al., 2010). We observed striking similarities between $Arc1^{18}$ mutants and *Sir2* mutants: in general, enzymes involved in fatty-acids synthesis and lipid accumulation were upregulated compared to their wt controls, and enzymes involved in lipid degradation and fatty acid oxidation were downregulated (Fig. 5B). Additionally, as in *Sir2* mutants, phosphoenolpyruvate carboxykinase (PEPCK), which is rate-limiting for gluconeogenesis and highly induced during starvation, was strongly repressed in $Arc1^{18}$ larvae (Fig. 5B). We conclude from these data that the absence of Arc1 results in widespread alterations in organismal energy homeostasis, leading to accumulation of excess energy stores.

2.7. Arc1 is required for E347 neuronal regulation of body fat

Our findings pointed to a fat-regulatory neuronal circuit involving E347 neurons and modulation of Arc1 levels in distinct neurons. Specifically, we hypothesized that upregulation of Arc1 is necessary for the lean phenotype observed upon E347 neuronal activation. To test this prediction, we activated E347 neurons in the presence or absence of Arc1. If Arc1 acts downstream of E347 activity, then loss of Arc1 should prevent the fat depletion observed upon E347 activation. In agreement with our model, larval density upon NB-mediated activation of E347 neurons was lower in an Arc1-null ($Arc1^{18}$) background than in a background-matched control ($Arc1^{115}$) (Fig. 6). Although we cannot rule out that loss of Arc1 increases body fat via a parallel, E347-independent pathway, this result strongly supports a model in which Arc1 is at least partially required for the lean phenotype observed upon E347 activation.

3. Discussion

There are multiple mechanisms by which neurons in the brain could regulate body fat. Signaling molecules produced both outside and within the CNS trigger specific neuronal responses in the brain, allowing the brain to coordinate processes that occur in distinct tissues, including the storage and usage of body fat. For example, insulin (or insulin-like peptides, in *Drosophila*) produced by the brain and other tissues is used to monitor nutritional status in order to maintain energy balance through regulation of food intake and levels of circulating carbohydrates (Geminard et al., 2009; Ikeya et al., 2002; Rulifson et al., 2002; Wu et al., 2005).

However, despite significant progress in understanding the specific regions of the brain responsible for coordinating the production and detection of relevant signaling molecules, we have only an incomplete picture of the various mechanisms that neurons use to control body fat levels.

Here we describe genetic dissection of a group of neurons within the CNS of the *Drosophila* larva that regulate fat storage. The E347 group of neurons expand from the MB, PI, SOG, optic lobes, and VNC (Fig. 3). Although this broad expression pattern might lead to a wide range of effects when E347 neurons are silenced or stimulated, our unbiased identification of Arc1 as a key factor in E347 control of body fat allows us to infer that the E347 neurons necessary for fat regulation are those that neighbor Arc1-expressing cells. However, we

cannot rule out that other, more distant E347 neurons, including those in other organs outside of the brain, are part of the same network and also required for fat regulation. Nonetheless, by pinpointing specific neuronal molecules acting in this process, our findings represent a major step forward in understanding the neuronal mechanisms of body fat regulation. By comparison, previous studies using similar *Drosophila* screens identified broadly-expressed groups of brain neurons that regulate body fat through modulation of food intake, metabolism, and gene expression in non-brain tissues (Al-Anzi et al., 2009) but did not characterize specific molecular effects of neuronal activity within the brain.

The Arc protein in mammals, also called Arg3.1, has been implicated in many molecular processes (Bramham et al., 2010), including control of cytoskeletal remodeling at post-synaptic dendrites (Huang et al., 2007), endocytosis of AMPA receptors (Chowdhury et al., 2006; Rial Verde et al., 2006; Shepherd et al., 2006; Tzingounis and Nicoll, 2006) and transcriptional accumulation in response to diverse learning tasks (Daberkow et al., 2007; Kelly and Deadwyler, 2002; Lonergan et al., 2010; Ramirez-Amaya et al., 2005). However, the precise mechanism by which Arc and its orthologs in other species regulate neuronal function remain unclear. Arc knockout mice are viable but cannot form long-lasting memories (Plath et al., 2006), pointing to a specific function for Arc in memory formation. Like other immediate early genes, Arc levels change significantly in response to synaptic activity (Lyford et al., 1995). Interestingly, relative to other immediate early genes rodent Arc is more highly induced during specific behaviors, particularly certain kinds of learning tasks (Guzowski et al., 2001; Lonergan et al., 2010). In brains of animals in which the synaptic activity of E347 neurons was experimentally activated, we found specific upregulation of Arc1 transcript relative to other immediate early genes, pointing to a specific role for Arc1 protein in body fat regulation downstream of E347 neurons.

We favor a model wherein E347 neurons make synapses with Arc1-expressing cells in the neurosecretory region of the mid-brain. While we did not detect an increase in the number of Arc1-expressing mid-brain cells upon E347 activation, the levels of Arc1 per cell may respond to E347 activity. In these cells, Arc1 could directly or indirectly induce fat depletion or inhibit fat storage in the FB.

The metabolic defects we observed in $Arc1^{18}$ mutant larvae do not allow us to distinguish between direct or indirect effects, but they do provide evidence of widespread alterations in organismal energy balance. Some trends emerge from further consideration of these changes. Higher levels of glycogen breakdown products indicate impaired energetics. However, despite higher availability of sugar substrates, $Arc1^{18}$ larvae displayed inefficient or partial oxidation of glucose through glycolysis and Krebs cycle, in favor of the accumulation of carbon backbone for *de novo* synthesis of storage lipids such as triglycerides. These findings provided strong independent support for the decreased density of $Arc1^{18}$ larvae revealed by our buoyancy assay.

Transcripts encoding PEPCK were reduced ~330 fold in $Arc1^{18}$ larvae (Fig. 5B). Misexpression of mouse PEPCK, which converts oxaloacetate to pyruvate, results in impaired glyceroneogenesis, while knock-down of liver isoforms results in severe impairment of Krebs cycle, accumulation of oxaloacetate, and fatty liver following fasting

(Beale et al., 2007). Excess oxaloacetate metabolism could, via transamination reactions mediated by glutamate oxaloacetate transaminase (GOT), be converted to aspartate, the highest statistically significant fold-change increase observed in *Arc1*^{18} larvae (Fig. 5A). Numerous other metabolic changes are also consistent with obesity, including increased glycogenolysis and glucose availability, decreased glucose oxidation at the Krebs cycle level (Felber et al., 1987), higher glycerol-phosphate generation (Neschen et al., 2005), increased activity of transaminases (elevated aspartate (Hanley et al., 2004)) and accumulation of BCAA, phenylalanine and tryosine (Adams, 2011).

In wt animals, Arc1 could directly regulate secretion of hormones or neuropeptides, via paracrine or endocrine signals, to promote fat depletion. Considering its known roles in synaptic plasticity, Arc1 could also act more indirectly to sensitize the cells that release fat regulatory signals to inputs from other regions of the brain. Arc1-triggered release of these putative signals must be independent of synaptic activity *per se*, because directly modifying synaptic activity in Arc1-expressing cells had no effect on organismal fat (data not shown). Accordingly, paracrine or endocrine signals are likely candidates for mediating downstream effects of E347 activity.

The differences upon modulation of E347 activity that we found in the numbers of Arc1-expressing cells in other parts of the brain may also have important functional consequences. Neurons in the SOG are associated with behaviors that respond to taste (Scott, 2005), and are in close proximity to the esophagus, which represents a physical connection between the brain and the gut (Melcher and Pankratz, 2005). However, Arc1 changes in the SOG presumably do not generally regulate these behaviors, because food intake was unaffected in animals in which we saw changes in Arc1. Instead, Arc1-expressing SOG cells could mediate sensing of nutritional inputs, facilitated by proximity to the esophagus. Interestingly, a high-fat diet causes a decrease in expression of mouse Arc in the cerebral cortex and hypothalamus, and a similar effect is observed in rat primary hippocampal neurons cultured with 27-hydroxycholesterol (Mateos et al., 2009).

We note that *Drosophila* Arc1 is responsible for a behavior that may be relevant to body fat control: wt adults exhibit a burst of locomotor activity upon starvation, whereas *Arc1* mutants are defective in this activity (Mattaliano et al., 2007). Despite lacking a normal response to starvation, however, *Arc1* adults are starvation resistant (Mattaliano et al., 2007), a phenotype that we can now attribute at least in part to excess fat stores. Interestingly, in *Drosophila* larvae clusters of insulin-like-peptide-producing cells (IPCs) in the brain are a major source of insulin during larval growth (Rulifson et al., 2002), and Arc1-expressing cells partially overlap with IPCs in adult brains (Mattaliano et al., 2007). Moreover, Arc1 expression restricted to IPCs restores normal starvation sensitivity, suggesting that Arc1 in IPCs is responsible for the starvation responses observed in wt adults (Mattaliano et al., 2007). Likewise, a rapid increase in Arc mRNA is observed in human neuroblast cells upon stimulation with insulin (Kremerskothen et al., 2002).

We thus favor a model in which starvation-induced insulin accumulation in IPCs (Geminard et al., 2009) upregulates Arc1, which stimulates release of signals promoting mobilization of energy stores, such as fat depletion. Indeed, although we did not detect transcriptional

changes for any of the *Drosophila* insulin-like peptides (Dilps) in our RNAseq analysis of E347 manipulation, we did notice by immunostaining that E347 silencing caused apparent accumulation of Dilp2 peptides within IPCs in the brain (unpublished data). Failure to secrete Dilps from IPCs could lead to a failure to upregulate Arc1 in the neurons in which Arc1 induction is under insulin control, possibly explaining the decreases in Arc1 expression we observed in the VNC and SOG upon E347 silencing. In further support of a role for Arc1 downstream, rather than upstream, of insulin signaling, in Arc^{18} larvae we did not observe significant changes by RT-qPCR in transcript levels of the insulin-responsive genes *inr* and *4ebp*, and found no difference in immunostaining of Dilp2 in IPCs (data not shown).

In summary, our findings identify a function for a widely-studied but poorly understood neuronal regulator, Arc1, in the regulation of body fat mediated by a specific group of neurons in the brain. Our data suggest that Arc has specific neuronal regulatory roles that extend beyond memory and learning.

4. Materials and methods

4.1. Fly strains and husbandry

W^{1118} (3605), *w;cg*-GAL4 (7011), y^1 w UAS-shi^{DN}; UAS-shi^{DN} (5811), y^1 w;+; UAS-NachBac (9469) and y^1 v^1;UAS-Arc1 RNAi (25954) we obtained from the Bloomington stock center. The neuronal GAL4 enhancer trap collection screened (including line E347) was obtained from Ulrike Heberlein. $Arc1^{115}$, $Arc1^{18}$, arc1-GAL4 and w; UAS-Arc1 were a generous gift from Leslie Griffith. Arc^{18} is null mutant resulting from an imprecise excision allele of a P-element insertion at the *Arc1* locus, which deletes the Arc1 coding sequence without affecting surrounding genes (Mattaliano et al., 2007). Arc^{115} is a precise excision allele that restores the full Arc1 coding sequence (Mattaliano et al., 2007). Larvae and flies were reared as previously described (Reis et al., 2010). E347-GAL4; $Arc1^{18}$, E347-GAL4; $Arc1^{115}$, w; $Arc1^{18}$; UAS-NB, w; $Arc1^{115}$; UAS-NB and E347-GAL4;+; UAS-GFP were generated using the available stocks.

4.2. Density assay

Density assays have been modified from previously described (Reis et al., 2010). Larvae were reared as previously described (Reis et al., 2010), and at the time of the assay all animals were at the same developmental stage and were floated to the top of the vial with 20% sucrose. Larvae were then transferred to a 50-ml conical tube containing 20.5 ml of 8.8% of sucrose and number of floating larvae was recorded. Increments of 1 ml of 20% sucrose were added, density equilibrium established and number of animals recorded again. At the end of the assay all animals were floated and total number recorded. Percent of floating animals was calculated by dividing the number of floating animals at a specific sucrose density by the total number of animals. Two-tailed paired t test was used to calculate statistical significance, using Prism 6 software.

4.3. Gas chromatography mass spectrometry

As previously described (Reis et al., 2010). Total neutral lipid extractions were analyzed using a Thermo Fisher Trace 1300-ISQ GC/MS system and weights measured using a

Mettler Toledo XS104 analytical scale. n = 5–8. Two-tailed paired t test was used to calculate statistical significance, using Prism 6 software.

4.4. Feeding assay

As previously described (Reis et al., 2010). Absorbances were measured using a Thermo scientific Evolution 60S spectrophometer. n=4. Two-tailed unpaired t test was used to calculate statistical significance, using Prism 6 software.

4.5. Activity assay

To measure levels of activity, eggs were collected on grape plates, allowed to eclose for 24 h at 25 °C, at which time first instar larvae were transferred to the experimental media. 4 days later, 15 pre-wandering third instar larvae were transferred to the center of a pre-warmed agar plate. 3 sets of 2-min-long movies were recorded. In between each movie, larvae were placed again in the center of the dish using a brush. For each experiment, the second of the 3 movies was used to analyze data. To measure movement and calculate velocities, larvae were automatically tracked using the wrMTrck plugin developed by Jesper S. Pedersen ⟨http://www. phage.dk/plugins/wrmtrck.html⟩, using the following parameters: minSize 20, maxSize 300, maxVelocity 10, maxAreaChange 40, minTrackLength 80, bendThreshold 2.0, FPS 30. n = 4. Two-tailed unpaired t test was used to calculate statistical significance, using Prism 6 software.

4.6. RNA-seq

We dissected 100 larval brains per genotype and isolated total RNA using Trizol (Life Technologies) reagent following the manufacturer's instructions. Polyadenylated RNA was isolated by oligodT purification, and strand-specific mRNA-seq libraries were prepared by cDNA conversion with random hexamers, second-strand synthesis in the presence of dUTP, ligation of double-stranded adapters, destruction of uracil-containing DNA with UDG followed by PCR amplification with indexed PCR primers (Levin et al., 2010). Libraries were pooled and single-end 50 bp sequences were collected on a HiSeq 2000. We aligned sequences to the Drosophila genome (dm3) with tophat2 (Kim et al., 2013) and compared mRNA abundances (FPKM) using the cufflinks package (Trapnell et al., 2013). Raw data (FASTQ) are available at NCBI GEO (Barrett et al., 2013) under accession GSE60822.

4.7. RT-qPCR

For each sample RNA was extracted from 80 brains or 10 larvae and processed as previously described (Reis et al., 2010). Two primer sets were used per target and levels normalized to an average of the levels of *actin5c, alpha-tubulin84B, cg5321 and cg12703*. Primer sequences: Arc1 primer pair 1: 5′ catcatcgagcacaacaacc 3′ and 5′ ctactcctcgtgctgctcct 3′ Arc1 primer pair 2: 5′ tcggtctgctgaacatcaag 3′ and 5′ gtgttctttgctgtggcaag 3′ jra primer pair 1: 5′ catttccgtccgccaattcc 3′ and 5′ catttccgtccgccaattcc 3′ jra primer pair 2: 5′ gcggtgaacaatggcatcag 3′ and 5′ tcctgcgcttccatgtcaat 3′ kay primer pair 1: 5′ caccatggccaacaacaagg 3′ and 5′ tgttcgtggaggagctgttc 3′ kay primer pair 2: 5′ cacaacagcaacgacagcag 3′ and 5′ ctggatcctgagtcgatggc 3′ act5c 5′ gagcgcggttactctttcac3′ and 5′ acttctccaacgaggagctg3′ tub84B 5′ aacctgaaccgtctgattgg 3’ and 5′ ggtcaccagagggaagtgaa 3′

cg5321 5′ taacttcgatacccgcatcc 3′ and 5′ cgaaacatcgctcctttagc 3′ cg12703 5′ tggtggagagcaccatcata 3′ and 5′ gcttcaactcacccaagctc 3′. Other primer sequences are provided elsewhere (Reis et al., 2010). Three independent biological replicates with respective RT and qPCR were performed. $n = 3$. Multiple comparisons ordinary one-way ANOVA was used to calculate statistical significance, using Prism 6 software.

4.8. Microscopy and cell counts

Wandering 3rd instar larvae were dissected and fixed with 4% paraformaldehyde (Electron Microscopy Sciences) O/N at 4 °C. Carcasses were then washed 3 times with 0.1% PBTriton and immunostaining performed as described (Reis et al., 2010). Arc1 antibody (Mattaliano et al., 2007) was used at a 1:500 dilution; GFP antibody (Roche) was diluted to 1:500. Notably, this Arc1 antibody has been tested extensively for specificity, and immunostaining signals are absent in -null animals ((Mattaliano et al., 2007) and our unpublished results). Secondary antibodies Alexa fluor anti-rabbit 568 (Invitrogen, Molecular Probes) and Alexa fluor anti-mouse 488 (Invitrogen, Molecular Probes) were used at 1:5000 dilution. Images were collected using a Leica TCS SP5 II confocal microscope. Cell counts were performed blind using a Nikon i80 microscope. Multiple t test comparison was used to calculate statistical significance, using Prism 6 software.

4.9. Oil Red O staining

Wandering 3rd instar larvae were dissected and fixed with 4% paraformaldehyde (Electron Microscopy Sciences) at RT for 30 min and washed 3 times with PBS containing 0.1% Triton. Carcasses were then washed twice in propylene glycol (Fisher, CAS 57556) for 15 min, and stained with 0.5% Oil Red O (Sigma, O-0625) for 20 min at 60 °C, inverting tubes every 5 min. Stained tissues were washed 3 times with 80% propylene glycol for 20 min, washed twice in PBS, and mounted in 80% glycerol.

4.10. Metabolomics

Metabolomics analyses were performed as previously reported (D'Alessandro et al., 2015; Nemkov et al., 2015). Briefly, 30 whole larvae, either $Arc1^{115}$ or $Arc1^{18}$ (n=10, biological experiment repeated 3 times; technical variability < 10% (Nemkov et al., 2015)) were homogenized (Bullet Blender Storm 24, Next Advance) and extracted at a 10 mg/ml ratio in ice-cold lysis/extraction buffer (methanol:acetonitrile:water 5:3:2). Water and methanol soluble fractions were run through a C18 reversed phase column (9 min gradient, phase A: water, 0.1% formic acid; B: acetonitrile, 0.1% formic acid) through an ultra-high performance HPLC system (Ultimate 3000, Thermo Fisher), coupled on line with a high resolution quadrupole Orbitrap instrument run in both polarity modes (QExactive, Thermo Fisher). Metabolite assignment and peak integration for relative quantitation were performed through the software Maven (Princeton), against the KEGG pathway database and an in-house validated standard library (> 650 compounds; SIGMA Aldrich; IROATech). Statistical elaboration for partial-least square-discriminant analysis (PLS-DA) and heat maps/hierarchical clustering analysis (HCA) was performed with the software MultiBase (Numerical Dynamics) and GENE E (Broad Institute). In Supplemental Table 1 we report metabolite names (KEGG IDs and pathway classification), analytical details (m/z, retention

times, integrated peak areas), and relative fold changes for each metabolite in either fat ($Arc1^{18}$) or wt larvae ($Arc1^{115}$), using two-tailed *t* tests for significance.

Supplementary Material

Refer to Web version on PubMed Central for supplementary material.

Acknowledgments

Kristin Scott and Iswar Hariharan provided key support in the early stages of this project. We also thank the Bloomington Stock Center for fly stocks, Ulrike Heberlein for kindly providing the enhancer trap collection, and Leslie Griffith for generously sharing the Arc1 fly stocks and Arc1 antibody. Michael McMurray, Kristin Scott and Abigail Person provided helpful feedback on the manuscript. This work was supported by NIH, NIDDK Grant 5K01DK095932 to T.R., AHA Award 12BGIA11930014 to T.R. and NIH/NCATS Colorado CTSA Grant UL1 TR001082 to K.C.H.

References

Adams SH. Emerging perspectives on essential amino acid metabolism in obesity and the insulin-resistant state. Adv. Nutr. 2011; 2:445–456. [PubMed: 22332087]

Al-Anzi B, Sapin V, Waters C, Zinn K, Wyman RJ, Benzer S. Obesity-blocking neurons in *Drosophila*. Neuron. 2009; 63:329–341. [PubMed: 19679073]

Anholt RR, Mackay TF. Genetics of aggression. Annu. Rev. Genet. 2012; 46:145–164. [PubMed: 22934647]

Baker KD, Thummel CS. Diabetic larvae and obese flies-emerging studies of metabolism in *Drosophila*. Cell Metab. 2007; 6:257–266. [PubMed: 17908555]

Barrett T, Wilhite SE, Ledoux P, Evangelista C, Kim IF, Tomashevsky M, Marshall KA, Phillippy KH, Sherman PM, Holko M, Yefanov A, Lee H, Zhang N, Robertson CL, Serova N, Davis S, Soboleva A. NCBI GEO: archive for functional genomics data sets–update. Nucleic Acids Res. 2013; 41:D991–D995. [PubMed: 23193258]

Beale EG, Harvey BJ, Forest C. PCK1 and PCK2 as candidate diabetes and obesity genes. Cell Biochem. Biophys. 2007; 48:89–95. [PubMed: 17709878]

Bramham CR, Alme MN, Bittins M, Kuipers SD, Nair RR, Pai B, Panja D, Schubert M, Soule J, Tiron A, Wibrand K. The Arc of synaptic memory. Exp. Brain Res. 2010; 200:125–140. [PubMed: 19690847]

Campos AR, Rosen DR, Robinow SN, White K. Molecular analysis of the locus elav in *Drosophila* melanogaster: a gene whose embryonic expression is neural specific. EMBO J. 1987; 6:425–431. [PubMed: 3107982]

Chowdhury S, Shepherd JD, Okuno H, Lyford G, Petralia RS, Plath N, Kuhl D, Huganir RL, Worley PF. Arc/Arg3.1 interacts with the endocytic machinery to regulate AMPA receptor trafficking. Neuron. 2006; 52:445–459. [PubMed: 17088211]

D'Alessandro A, Moore HB, Moore EE, Wither M, Nemkov T, Gonzalez E, Slaughter A, Fragoso M, Hansen KC, Silliman CC, Banerjee A. Early hemorrhage triggers metabolic responses that build up during prolonged shock. Am. J. Physiol. Regul. Integr. Comp. Physiol. 2015; 308:R1034–R1044. [PubMed: 25876652]

Daberkow DP, Riedy MD, Kesner RP, Keefe KA. Arc mRNA induction in striatal efferent neurons associated with response learning. Eur. J. Neurosci. 2007; 26:228–241. [PubMed: 17614950]

Davis RL. Traces of *Drosophila* memory. Neuron. 2011; 70:8–19. [PubMed: 21482352]

Felber JP, Ferrannini E, Golay A, Meyer HU, Theibaud D, Curchod B, Maeder E, Jequier E, DeFronzo RA. Role of lipid oxidation in pathogenesis of insulin resistance of obesity and type II diabetes. Diabetes. 1987; 36:1341–1350. [PubMed: 3311856]

Geminard C, Rulifson EJ, Leopold P. Remote control of insulin secretion by fat cells in *Drosophila*. Cell Metab. 2009; 10:199–207. [PubMed: 19723496]

Goldstein ES, Treadway SL, Stephenson AE, Gramstad GD, Keilty A, Kirsch L, Imperial M, Guest S, Hudson SG, LaBell AA, O'Day M, Duncan C, Tallman M, Cattelino A, Lim J. A genetic analysis of the cytological region 46 C-F containing the *Drosophila* melanogaster homolog of the jun proto-oncogene. Mol. Genet. Genomics: MGG. 2001; 266:695–700. [PubMed: 11810242]

Gordon MD, Scott K. Motor control in a *Drosophila* taste circuit. Neuron. 2009; 61:373–384. [PubMed: 19217375]

Guh DP, Zhang W, Bansback N, Amarsi Z, Birmingham CL, Anis AH. The incidence of co-morbidities related to obesity and overweight: a systematic review and meta-analysis. BMC Public Health. 2009; 9:88. [PubMed: 19320986]

Guzowski JF, Setlow B, Wagner EK, McGaugh JL. Experience-dependent gene expression in the rat hippocampus after spatial learning: a comparison of the immediate-early genes Arc, c-fos, and zif268. J. Neurosci.: Off. J. Soc. Neurosci. 2001; 21:5089–5098.

Hanley AJ, Williams K, Festa A, Wagenknecht LE, D'Agostino RB Jr. Kempf J, Zinman B, Haffner SM. Elevations in markers of liver injury and risk of type 2 diabetes: the insulin resistance atherosclerosis study. Diabetes. 2004; 53:2623–2632. [PubMed: 15448093]

Huang F, Chotiner JK, Steward O. Actin polymerization and ERK phosphorylation are required for Arc/Arg3.1 mRNA targeting to activated synaptic sites on dendrites. J. Neurosci.: Off. J. Soc. Neurosci. 2007; 27:9054–9067.

Hudson SG, Garrett MJ, Carlson JW, Micklem G, Celniker SE, Goldstein ES, Newfeld SJ. Phylogenetic and genomewide analyses suggest a functional relationship between kayak, the *Drosophila* fos homolog, and fig, a predicted protein phosphatase 2 c nested within a kayak intron. Genetics. 2007; 177:1349–1361. [PubMed: 18039871]

Ikeya T, Galic M, Belawat P, Nairz K, Hafen E. Nutrient-dependent expression of insulin-like peptides from neuroendocrine cells in the CNS contributes to growth regulation in *Drosophila*. Curr. Biol.: CB. 2002; 12:1293–1300. [PubMed: 12176357]

Kaun KR, Devineni AV, Heberlein U. Drosophila melanogaster as a model to study drug addiction. Hum. Genet. 2012; 131:959–975. [PubMed: 22350798]

Kelly MP, Deadwyler SA. Acquisition of a novel behavior induces higher levels of Arc mRNA than does overtrained performance. Neuroscience. 2002; 110:617–626. [PubMed: 11934470]

Kim D, Pertea G, Trapnell C, Pimentel H, Kelley R, Salzberg SL. TopHat2: accurate alignment of transcriptomes in the presence of insertions, deletions and gene fusions. Genome Biol. 2013; 14:R36. [PubMed: 23618408]

Kitamoto T. Conditional modification of behavior in *Drosophila* by targeted expression of a temperature-sensitive shibire allele in defined neurons. J. Neurobiol. 2001; 47:81–92. [PubMed: 11291099]

Kremerskothen J, Wendholt D, Teber I, Barnekow A. Insulin-induced expression of the activity-regulated cytoskeleton-associated gene (ARC) in human neuroblastoma cells requires p21(ras), mitogen-activated protein kinase/extracellular regulated kinase and src tyrosine kinases but is protein kinase C-independent. Neurosci. Lett. 2002; 321:153–156. [PubMed: 11880195]

Levin JZ, Yassour M, Adiconis X, Nusbaum C, Thompson DA, Friedman N, Gnirke A, Regev A. Comprehensive comparative analysis of strand-specific RNA sequencing methods. Nat. Methods. 2010; 7:709–715. [PubMed: 20711195]

Li HH, Kroll JR, Lennox SM, Ogundeyi O, Jeter J, Depasquale G, Truman JW. A GAL4 driver resource for developmental and behavioral studies on the larval CNS of *Drosophila*. Cell Rep. 2014; 8:897–908. [PubMed: 25088417]

Lonergan ME, Gafford GM, Jarome TJ, Helmstetter FJ. Time-dependent expression of Arc and zif268 after acquisition of fear conditioning. Neural Plast. 2010; 2010:139891. [PubMed: 20592749]

Luan H, Lemon WC, Peabody NC, Pohl JB, Zelensky PK, Wang D, Nitabach MN, Holmes TC, White BH. Functional dissection of a neuronal network required for cuticle tanning and wing expansion in *Drosophila*. J. Neurosci.: Off. J. Soc. Neurosci. 2006; 26:573–584.

Lyford GL, Yamagata K, Kaufmann WE, Barnes CA, Sanders LK, Copeland NG, Gilbert DJ, Jenkins NA, Lanahan AA, Worley PF. Arc, a growth factor and activity-regulated gene, encodes a novel cytoskeleton-associated protein that is enriched in neuronal dendrites. Neuron. 1995; 14:433–445. [PubMed: 7857651]

Mateos L, Akterin S, Gil-Bea FJ, Spulber S, Rahman A, Bjorkhem I, Schultzberg M, Flores-Morales A, Cedazo-Minguez A. Activity-regulated cytoskeleton-associated protein in rodent brain is down-regulated by high fat diet in vivo and by 27-hydroxycholesterol in vitro. Brain Pathol. 2009; 19:69–80. [PubMed: 18503570]

Mattaliano MD, Montana ES, Parisky KM, Littleton JT, Griffith LC. The *Drosophila* ARC homolog regulates behavioral responses to starvation. Mol. Cell Neurosci. 2007; 36:211–221. [PubMed: 17707655]

Melcher C, Pankratz MJ. Candidate gustatory interneurons modulating feeding behavior in the Drosophila brain. PLoS Biol. 2005; 3:e305. [PubMed: 16122349]

Moline MM, Southern C, Bejsovec A. Directionality of wingless protein transport influences epidermal patterning in the *Drosophila* embryo. Development. 1999; 126:4375–4384. [PubMed: 10477304]

Morton GJ, Cummings DE, Baskin DG, Barsh GS, Schwartz MW. Central nervous system control of food intake and body weight. Nature. 2006; 443:289–295. [PubMed: 16988703]

Nemkov T, D'Alessandro A, Hansen KC. Three-minute method for amino acid analysis by UHPLC and high-resolution quadrupole orbitrap mass spec-trometry. Amino Acids. 2015

Neschen S, Morino K, Hammond LE, Zhang D, Liu ZX, Romanelli AJ, Cline GW, Pongratz RL, Zhang XM, Choi CS, Coleman RA, Shulman GI. Prevention of hepatic steatosis and hepatic insulin resistance in mitochondrial acyl-CoA:glycerol-sn-3-phosphate acyltransferase 1 knockout mice. Cell Metab. 2005; 2:55–65. [PubMed: 16054099]

Plath N, Ohana O, Dammermann B, Errington ML, Schmitz D, Gross C, Mao X, Engelsberg A, Mahlke C, Welzl H, Kobalz U, Stawrakakis A, Fernandez E, Waltereit R, Bick-Sander A, Therstappen E, Cooke SF, Blanquet V, Wurst W, Salmen B, Bosl MR, Lipp HP, Grant SG, Bliss TV, Wolfer DP, Kuhl D. Arc/Arg3.1 is essential for the consolidation of synaptic plasticity and memories. Neuron. 2006; 52:437–444. [PubMed: 17088210]

Pospisilik JA, Schramek D, Schnidar H, Cronin SJ, Nehme NT, Zhang X, Knauf C, Cani PD, Aumayr K, Todoric J, Bayer M, Haschemi A, Puviindran V, Tar K, Orthofer M, Neely GG, Dietzl G, Manoukian A, Funovics M, Prager G, Wagner O, Ferrandon D, Aberger F, Hui CC, Esterbauer H, Penninger JM. Drosophila genome-wide obesity screen reveals hedgehog as a determinant of brown versus white adipose cell fate. Cell. 2010; 140:148–160. [PubMed: 20074523]

Ramirez-Amaya V, Vazdarjanova A, Mikhael D, Rosi S, Worley PF, Barnes CA. Spatial exploration-induced Arc mRNA and protein expression: evidence for selective, network-specific reactivation. J. Neurosci.: Off. J. Soc. Neurosci. 2005; 25:1761–1768.

Ramirez-Zacarias JL, Castro-Munozledo F, Kuri-Harcuch W. Quantitation of adipose conversion and triglycerides by staining intracytoplasmic lipids with Oil red O. Histochemistry. 1992; 97:493–497. [PubMed: 1385366]

Reis T, Van Gilst MR, Hariharan IK. A buoyancy-based screen of Drosophila larvae for fat-storage mutants reveals a role for Sir2 in coupling fat storage to nutrient availability. PLoS Genet. 2010; 6:e1001206. [PubMed: 21085633]

Ren D, Navarro B, Xu H, Yue L, Shi Q, Clapham DE. A prokaryotic voltage-gated sodium channel. Science. 2001; 294:2372–2375. [PubMed: 11743207]

Rial Verde EM, Lee-Osbourne J, Worley PF, Malinow R, Cline HT. Increased expression of the immediate-early gene arc/arg3.1 reduces AMPA receptor-mediated synaptic transmission. Neuron. 2006; 52:461–474. [PubMed: 17088212]

Rulifson EJ, Kim SK, Nusse R. Ablation of insulin-producing neurons in flies: growth and diabetic phenotypes. Science. 2002; 296:1118–1120. [PubMed: 12004130]

Scott K. Taste recognition: food for thought. Neuron. 2005; 48:455–464. [PubMed: 16269362]

Shepherd JD, Rumbaugh G, Wu J, Chowdhury S, Plath N, Kuhl D, Huganir RL, Worley PF. Arc/Arg3.1 mediates homeostatic synaptic scaling of AMPA receptors. Neuron. 2006; 52:475–484. [PubMed: 17088213]

Thorleifsson G, Walters GB, Gudbjartsson DF, Steinthorsdottir V, Sulem P, Helgadottir A, Styrkarsdottir U, Gretarsdottir S, Thorlacius S, Jonsdottir I, Jonsdottir T, Olafsdottir EJ, Olafsdottir GH, Jonsson T, Jonsson F, Borch-Johnsen K, Hansen T, Andersen G, Jorgensen T, Lauritzen T, Aben KK, Verbeek AL, Roeleveld N, Kampman E, Yanek LR, Becker LC,

Tryggvadottir L, Rafnar T, Becker DM, Gulcher J, Kiemeney LA, Pedersen O, Kong A, Thorsteinsdottir U, Stefansson K. Genome-wide association yields new sequence variants at seven loci that associate with measures of obesity. Nat. Genet. 2009; 41:18–24. [PubMed: 19079260]

Trapnell C, Hendrickson DG, Sauvageau M, Goff L, Rinn JL, Pachter L. Differential analysis of gene regulation at transcript resolution with RNA-seq. Nat. Biotechnol. 2013; 31:46–53. [PubMed: 23222703]

Tzingounis AV, Nicoll RA. Arc/Arg3.1: linking gene expression to synaptic plasticity and memory. Neuron. 2006; 52:403–407. [PubMed: 17088207]

Wu Q, Zhang Y, Xu J, Shen P. Regulation of hunger-driven behaviors by neural ribosomal S6 kinase in Drosophila. Proc. Natl. Acad. Sci. USA. 2005; 102:13289–13294. [PubMed: 16150727]

Yamamoto D, Koganezawa M. Genes and circuits of courtship behaviour in *Drosophila* males. Nat. Rev. Neurosci. 2013; 14:681–692. [PubMed: 24052176]

Author summary

As obesity reaches near-epidemic proportions, it becomes increasingly important to identify specific regions of the brain that act as control centers for fat storage, and the gene products involved in this control. The fruit fly has been a powerful model system both for dissecting neuronal roles in brain function, and identifying the functions of specific genes, most of which have obvious counterparts in humans. We performed an unbiased search for groups of neurons whose activity is required to prevent fly larvae from accumulating body fat. Among these, we determined which deplete body fat when experimentally activated. We then focused on one set of neurons (called E347) and performed an unbiased search for genes that are turned on in the brain upon neuronal activation, and turned off upon neuronal inhibition. Strikingly, one such gene, *Arc1*, we had already found in a previous search for fat mutant larvae, and its human counterpart is known to regulate learning and memory. Metabolic alterations in *Arc1* mutants support a shift towards energy storage. We discovered that Arc1 is turned on in neurons that are distinct from, but in close proximity to, the E347 neurons, and is important for the brain's ability to regulate body fat storage. These findings will help understanding of the brain's role in preventing obesity.

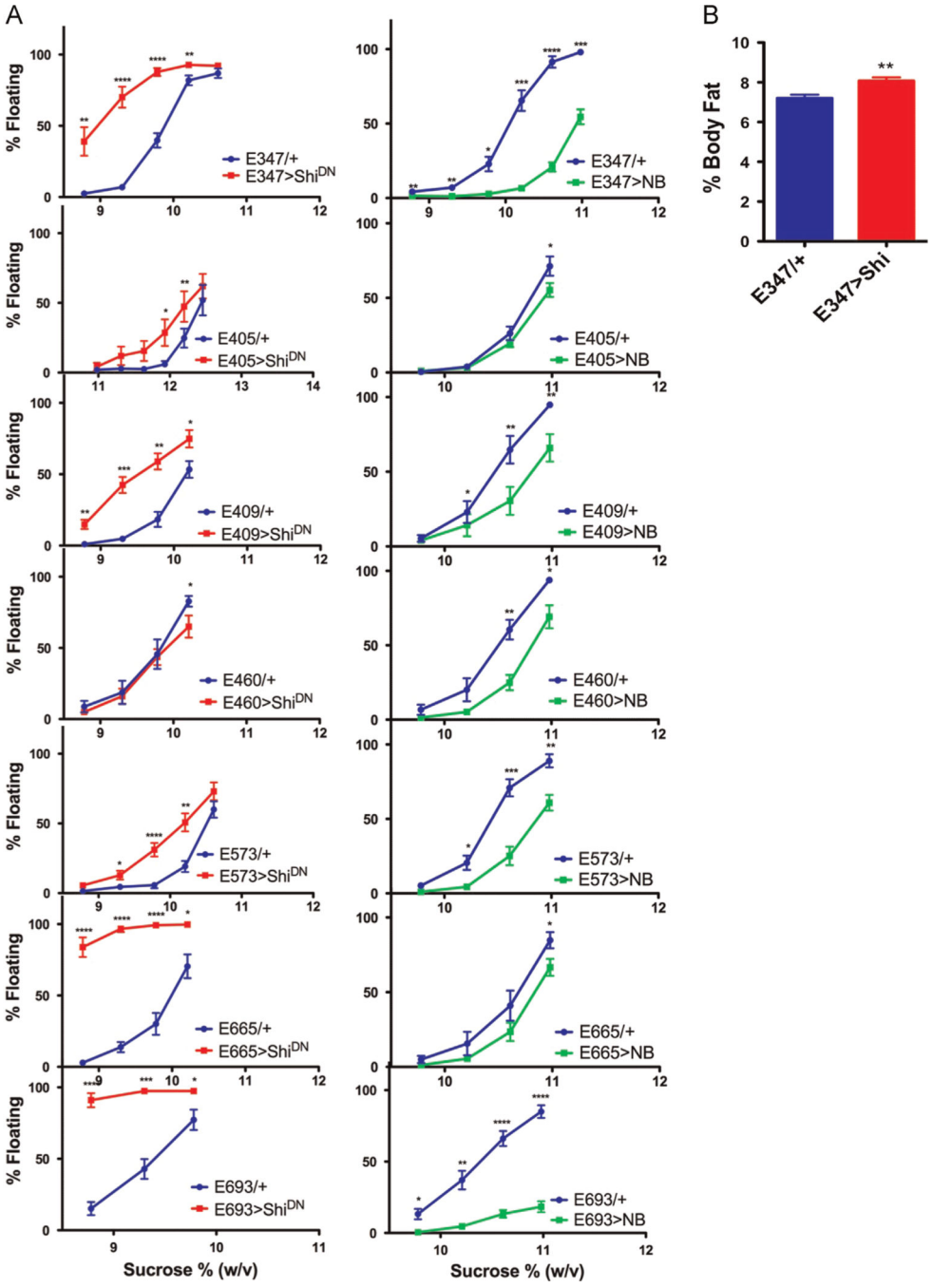

Fig. 1.

Neuronal function in specific regions of the larval brain is necessary and sufficient for body fat regulation. Neuronal activity in the indicated GAL4 lines was silenced by overexpression of Shi^{DN}, or activated by overexpression of NB, as indicated in the panels, and effects on body fat were assessed. (A) Percent of floating larvae at equilibrium in different density solutions. 50 larvae were examined per biological replicate, *n*=7–9 biological replicates per genotype. (B) Percent body fat (total neutral lipids divided by body weight) as measured by GCMS (*n*=8). Blue lines or bars represent GAL4-only (no UAS) animals crossed to w^{1118} to

control for effects of genetic background. *P* values represent results from two-tailed *t* tests. **** *P* <0.0001, *** *P* 0.0001–0.001, ** *P* 0.001–0.01, * *P* 0.01–0.05.

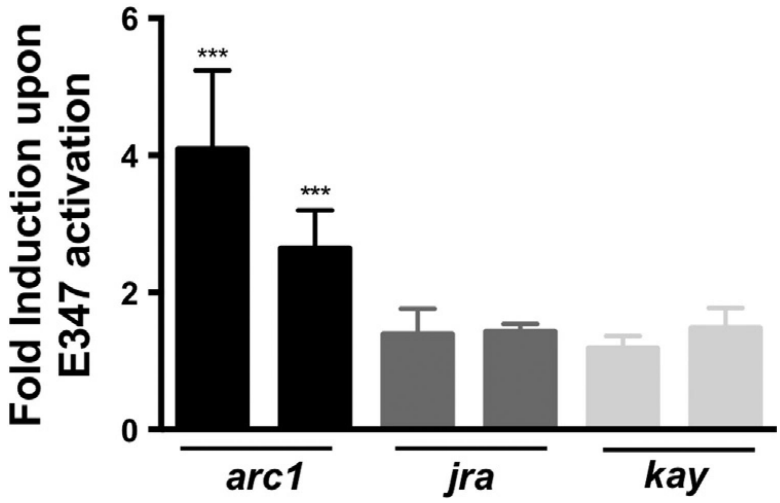

Fig. 2.

Induction of Arc1 upon E347 neuronal stimulation. The indicated transcripts were detected by quantitative RT-PCR from brains of wandering larvae. Each target transcript was detected with two distinct primer pairs and normalized to transcript levels of *actin5c*, *alpha-tubulin84B*, *cg5321* and *cg12703* (see Materials and methods). Shown are fold inductions of levels in E347 > NB brains (activation) versus E347/+ brains (no manipulation). *n*=3, Ordinary One-Way ANOVA was used to calculate statistical significance. *** $0.0001 < P < 0.001$.

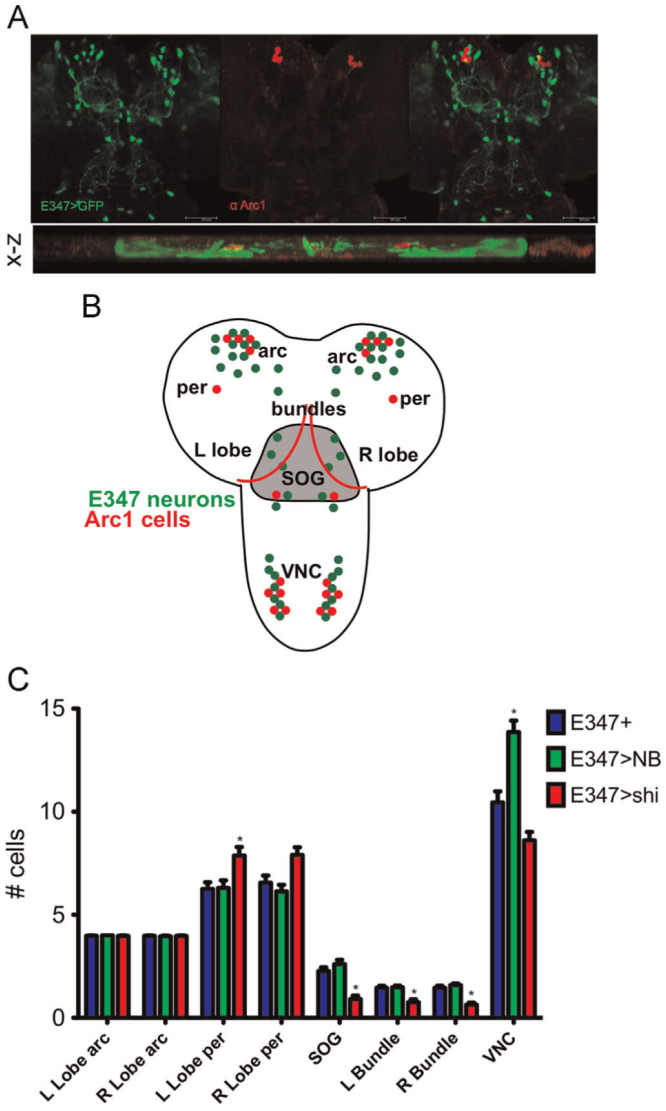

Fig. 3.

Arc1 expression in cells proximal to E347 neurons is dependent on E347 neuronal activity. (A) Immunostaining of E347 > GFP brains: green or red show anti-GFP or anti-Arc1 antibodies, respectively. Arc1-expressing cells are proximal to but distinct from 347 > GFP cells. The image below shows an "*x–z*" view of the brain using a composite of a *z*-series of 0.46 μm intervals. (B) Schematic of larval brain with E347 neurons represented as green dots and Arc1 cells as red dots. "arc" regions indicates the previously characterized regions in which Arc1 is expressed (Mattaliano et al., 2007); per, the Arc1-expressing peripheral cells; bundles, a subset of neuronal bundles in the mid region of the brain; L or R lobe, left or right lobe; SOG, subesophageal ganglion; VNC, ventral nerve cord. (C) The number of Arc1-expressing cells in each region in (B) was counted in immunostained brains of the indicated genotypes. n=33–38, counts were performed blind. Multiple t test comparison was used to calculate significance. *P 0.01–0.05.

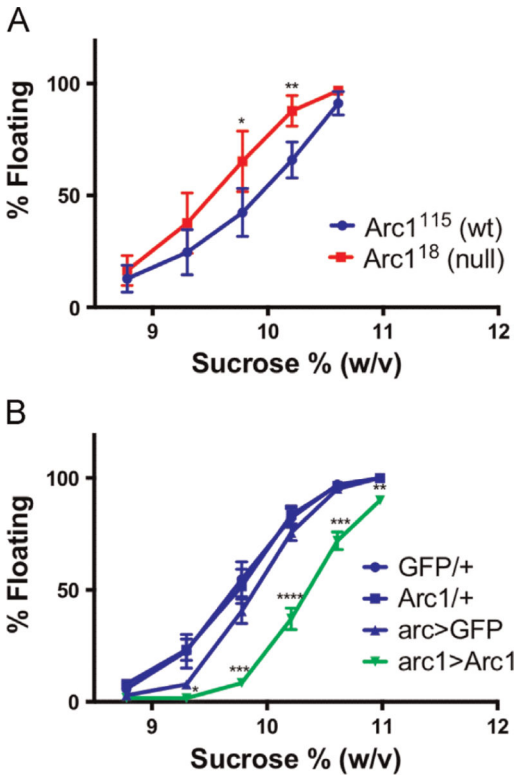

Fig. 4.

Arc1 is necessary and sufficient for depletion of body fat. As in Fig. 1A, for (A) *Arc*^{18} null mutants versus the *Arc*^{115} wt genetic background control. *n*=5, or (B) Arc1 overexpression under the arc-GAL4 promoter. *n*=8. Overexpression of GFP (arc > GFP) was used as a control.

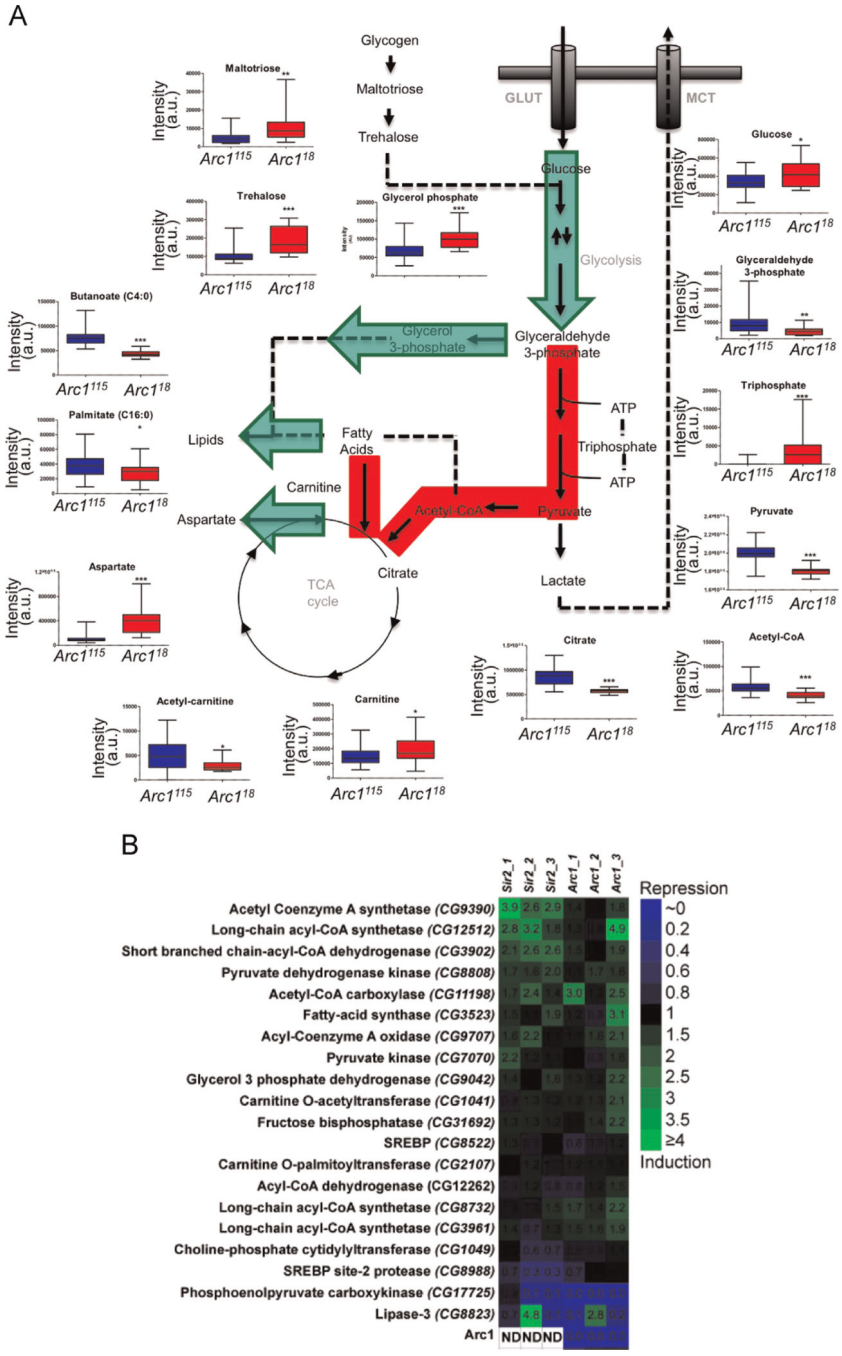

Fig. 5.

Metabolic alterations in *Arc1* mutant larvae. (A) Quantification of selected metabolites by UPLC of 30 individual larvae of each of the indicated genotypes, where $Arc1^{115}$ is a wt control and $Arc1^{18}$ is a loss-of-function mutant allele. Results are graphed as box plots, indicating mean values (lines) and upper/lower quartile distributions for each group. Asterisks indicate significance upon paired two-tailed *t* test (*, $P < 0.1$; **, $P < 0.01$; ***, $P < 0.001$). Selected pathways are illustrated with large green arrows indicating upregulation in $Arc1^{18}$ mutants, whereas downregulated pathways are highlighted in red. “GLUT”,

glucose transporter; “MCT”, monocarboxylate transporter; a.u., arbitrary units. (B) Heat maps illustrate changes in transcript levels of the indicated metabolic enzymes in *Arc1*^{18} compared to control *Arc1*^{115} larvae, as assessed by qRT-PCR. Each column represents an independent sample of 10 larvae. For comparison, published data (Reis et al., 2010) from the same transcripts in *Sir2* mutant larvae are shown. *Arc1* transcripts were undetectable in the *Arc1*^{18} larvae, as expected, ND, not determined.

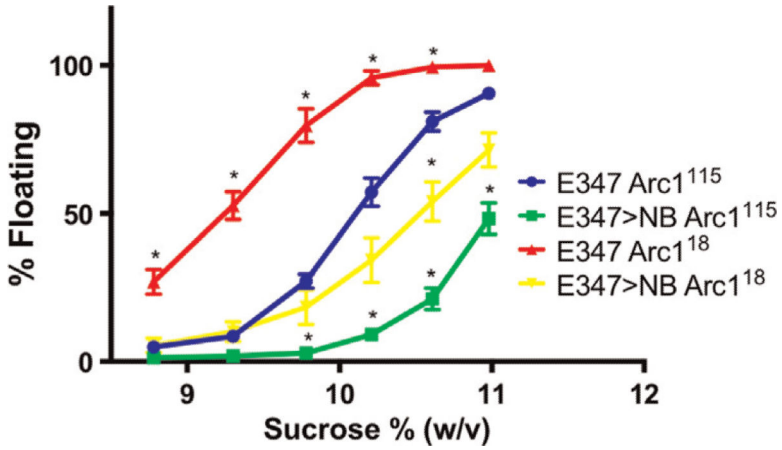

Fig. 6.

Arc1 is required for the decreased body fat observed upon E347-neuronal activation. As in Fig. 1A, for E347- neuronal driver in an Arc^{115} wt background (E347Arc^{115}) compared to E347-NB neuronal activation in the same background (E347 > NB Arc^{115}) or in an Arc^{18} null mutant background (E347 > NB Arc^{18}). (E347 Arc^{18}), E347 neuronal driver alone in Arc^{18}-mutant background. n=8, 50 larvae per biological replicate. Paired two-tailed t test was used to calculate significance. *$P \leq 0.05$, compared to 347 $Arc1^{115}$ control. Comparing E347 > NB^{15} to E347 > NB Arc^{18} with the same analysis, significant ($P \leq 0.05$) differences were observed for all densities except 8.78%.

Table 1

Neuronal enhancer-trap line	Buoyancy (8% sucrose)	Region of expression[a]
Oregon-R	-	Wt control (no expression)
E66, E447*, E454, E468, E558, E560,	+++	Ubiquitous
E67*	+++	MB, VNC
E145	+++	PI, SOG, VNC, other
E401, E413, E513, E782, E785	+++	Central brain, VNC
E409*	+++	Central brain, SOG, VNC
E440*	+++	Central brain, SOG, VNC, other
E477, E665*	+++	SOG, VNC
E527	+++	MB, PI, SOG, VNC
E533	+++	Glia
E52, E693*	++	SOG, VNC, other
E63, E405*, E411, E444, E573*	++	SOG, VNC
E127, E406, E416	++	PI, SOG, VNC
E323	++	MB, PI, VNC, other
E339	++	PI, SOG, VNC, other
E342*, E419*, E485	++	Glia
E408, E427, E472, E459, E538, E619, E775, E777	++	Central brain, VNC
E488*	++	SOG, other
E545*	++	PI, VNC, other
E633, E710	++	MB, VNC
E237, E347*	+	MB, PI, SOG, VNC
E348, E709, E812	+	Central brain, VNC
E461	+	PI
E466	+	PI, SOG
E491, E603, E670, E783*, E787	+	ubiquitous
E602, E739	+	Optic lobe, other
E685	+	Glia
E712, E766	+	MB, VNC

*14 lines chosen as representative and/or more restricted patterns of expression used on secondary screening.

[a]According to localization of GFP in brains dissected from larvae in which the GAL4 enhancer-trap line was used to drive expression of UAS-linked GFP. Wt, wild-type; SOG, subesophageal ganglion; VNC, ventral nerve cord; MB, mushroom body; PI, Pars intercerebralis.